

# A Hybrid Monte Carlo-S<sub>2</sub> Method for Neutron Transport with No Spatial Truncation Error

Emily R. Wolters

Department of Nuclear Engineering & Radiological Sciences  
University of Michigan, Ann Arbor, Michigan

*July 28, 2009*

*Oak Ridge National Laboratory, Oak Ridge, Tennessee*

# Outline

1. Introduction
2. Computational Issues with Transport Effects
3. Derivation of the Hybrid Equations
4. How to Solve the Hybrid Equations
5. Why Not Standard Monte Carlo?
6. Test Problem & Numerical Results
7. Comparison with Standard Monte Carlo and Deterministic Results
8. Conclusions
9. Future Work

# Introduction

## Personal:

- Doctoral Candidate, Nuclear Engineering & Radiological Sciences, University of Michigan, Ann Arbor, Michigan
- Research Area: Computational Methods for Neutron Transport
- Research Advisors: Ed Larsen & Bill Martin

## About this work:

- **Hybrid (deterministic + stochastic)** methods are recently being considered with interest for reactor physics problems
- U-M researching hybrid methods for radiation transport problems
- This work formulated for problems with significant transport effects
- Previous related work [1] presented at the 2009 M&C in Saratoga Springs, NY
- New work to be presented at 2009 ANS Winter Meeting in Washington, DC

# Transport Effects

## What are transport effects?

- **Features of the solution not preserved by numerical approximations to the transport equation** (i.e., multigroup vs. continuous energy)
- Often occur near material interfaces/boundaries

## Conventional computational methods may be inadequate for solving problems with transport effects. Some issues include:

- Deterministic: discretization errors, multigroup approximation, ray effects

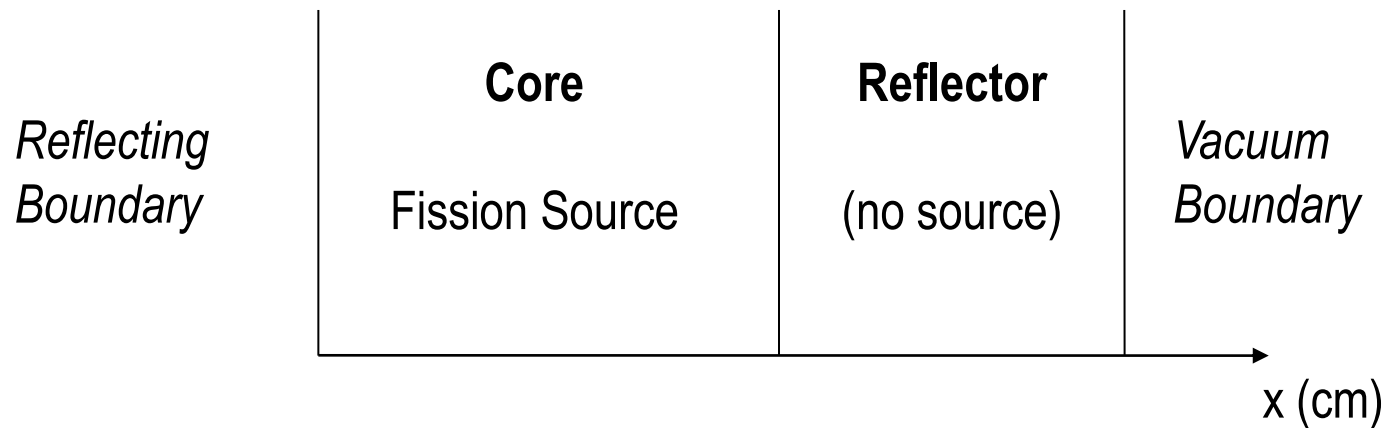
## We have developed a new method for such problems with the focus of simultaneously reducing errors in angle, energy and space.

- Hybrid Monte Carlo-deterministic
- No approximation in energy, angle, or space
- Small statistical errors
- Less expensive than standard Monte Carlo

# Transport Effects (continued)

**Aliberti, et al. (2004) & Lebrat , et al. (2002) analyzed a model reflected fast reactor using  $MGS_N$ .**

- Coupled energy-angle dependence of the flux near core-reflector interface
- 300+ groups needed for accurate reaction rate results near interface
- 33 groups acceptable if material regions are subdivided near interface and accurate spectra computed in each region for multigroup collapse



# Transport Effects (continued)

Issues are caused by the multigroup approximation.

$$\Sigma_{t,g}(\vec{r}, \hat{\Omega}) \equiv \frac{\int_{E_g}^{E_{g-1}} dE \Sigma_t(\vec{r}, E) \psi(\vec{r}, \hat{\Omega}, E)}{\int_{E_g}^{E_{g-1}} dE \psi(\vec{r}, \hat{\Omega}, E)} \longrightarrow \Sigma_{t,g}^i = \frac{\int_{E_g}^{E_{g-1}} dE \Sigma_t^i(E) \phi_{approx}^i(E)}{\int_{E_g}^{E_{g-1}} dE \phi_{approx}^i(E)}$$

- Rigorous collapse: continuous function of space and angle
- Multigroup collapse: constant in each spatial region, isotropic weighting fcn
- Replacing angular flux with approximate spectrum to eliminate angular dependence results in loss of important information
- Mitigated if a very fine energy grid is used and/or the group constants are defined over refined spatial regions

**How do we derive low-order equations (like MGS<sub>N</sub>) that are accurate in energy, angle and space?**

**What are the advantages of doing this?**

# Hybrid Method – Overview

- I. Reduce the exact transport equation to “low-order” equations containing special nonlinear functionals rather than multigroup cross sections.
- II. Determine the functionals with continuous-energy Monte Carlo.
- III. Solve the low-order equations with a modified discrete ordinates method resembling one-group  $S_2$ .

**Hybrid Method:** If the hybrid method functionals are known exactly, the low-order equations have no energy, angular, or spatial truncation errors.

**Multigroup Methods:** Even if the multigroup cross sections are known exactly, the low-order equations still have energy, angular, and spatial truncation errors (except for infinite medium problems).

# Hybrid Method – Starting Point

## 1-D Planar Geometry Transport Equation with B.C.s

- isotropic scattering and source
- no fission, inelastic scattering or upscattering

$$\mu \frac{\partial}{\partial x} \psi(x, \mu, E) + \Sigma_t(x, E) \psi(x, \mu, E) \tag{1a}$$

$$= \frac{1}{2} \int_0^\infty dE' \Sigma_s(x, E') p(x, E' \rightarrow E) \phi(x, E') + \frac{1}{2} Q(x, E)$$

$$\text{Left Reflecting BC} \longrightarrow \psi(0, \mu, E) = \psi(0, -\mu, E), \quad \mu > 0, \quad 0 < E < \infty \tag{1b}$$

$$\text{Right Incoming BC} \longrightarrow \psi(X, \mu, E) = \psi^R(\mu, E), \quad \mu < 0, \quad 0 < E < \infty \tag{1c}$$

### Goal: Compute response, $R(x)$

- Must be chosen *a priori* (no post-processing)

$$R(x) = \int_0^\infty dE r(x, E) \phi(x, E) \tag{2}$$

# Key Idea: Incorporate Angular Dependence

Introduce the following notation for “left” and “right” angularly integrated quantities:

$$\psi^\pm(x, E) \equiv \pm \int_0^{\pm 1} d\mu \psi(x, \mu, E) \quad (3a)$$

$$\longrightarrow \phi(x, E) = \psi^-(x, E) + \psi^+(x, E) \quad (3b)$$

$$R^\pm(x) \equiv \pm \int_0^\infty dE \int_0^{\pm 1} d\mu r(x, E) \psi(x, \mu, E) \quad (4a)$$

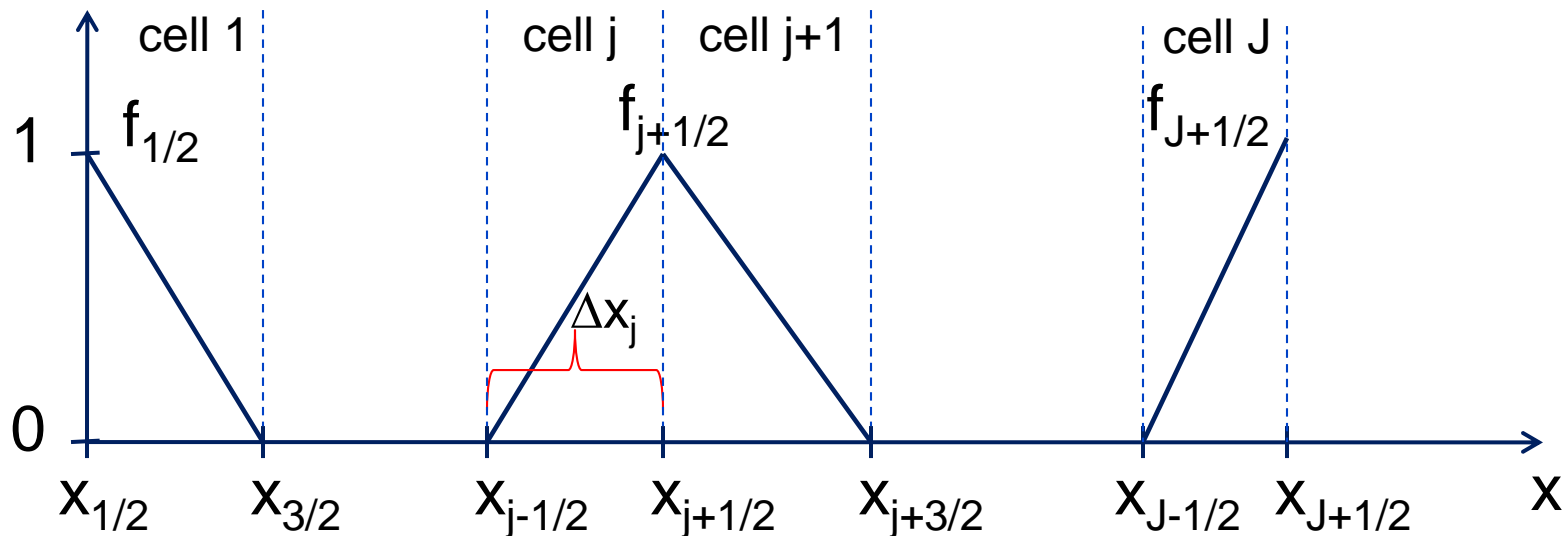
$$\longrightarrow R(x) = R^-(x) + R^+(x) \quad (4b)$$

Reaction rates at  $x$  due to neutrons traveling left and right

In this method, we will derive low-order equations for the half-range reaction rates.

# Derivation of the Low-Order Equations

1. Introduce a spatial mesh of  $J$  cells over the slab.
  - Arbitrary mesh spacing
  - Cells ordered  $0 = x_{1/2} < \dots < x_{j-1/2} < x_{j+1/2} < \dots < x_{J+1/2} = X$
  - Cells  $j=2 \dots J-1$  are interior cells; cell 1 and cell  $J$  are boundary cells
2. Define the  $J+1$  tent functions,  $f_{j+1/2}(x)$  ( $j=0, \dots, J$ ).



# Derivation (continued)

3. Apply the following operators to the transport equation.

$$F_{j+1/2}^{\pm}(\cdot) = \pm \int_0^{\pm 1} \int_0^X \int_0^{\infty} f_{j+1/2}(x)(\cdot) dE dx d\mu \quad (5)$$

These operators (1) Multiply the transport equation by the  $j^{\text{th}}$  tent function, and (2) Integrate over all space, all energy, and direction half-ranges ( $\mu > 0$  and  $\mu < 0$ ).

In [1], we applied a different operator that (1) Multiplied the transport equation by a histogram function, and (2) Integrated over the same phase space. This resulted in a different system of equations with spatial truncation error.

4. Simplify the leakage term using tent function properties.
5. Multiply each term by a “convenient” factor of unity to define functionals.

# Leakage Term

Here we demonstrate how the operator acts on the leakage term.

For the interior cells:

$$\pm \int_0^X \int_0^\infty \int_0^{\pm 1} f_{j+1/2}(x) \left[ \mu \frac{d}{dx} \psi(x, \mu, E) \right] d\mu dE dx = \int_{\Delta x_j + \Delta x_{j+1}} f_{j+1/2}(x) \frac{d}{dx} J^\pm(x) dx$$

$$J^\pm(x) = \pm \int_0^\infty \int_0^{\pm 1} \mu \psi(x, \mu, E) d\mu dE dx$$

1. Separate this term into two integrals

$$= \int_{\Delta x_j} f_{j+1/2}(x) \frac{d}{dx} J^\pm(x) dx + \int_{\Delta x_{j+1}} f_{j+1/2}(x) \frac{d}{dx} J^\pm(x) dx$$

2. Integrate by parts.

- $f_{j+1/2}(x)$  is 0 or 1 at cell edges
- $\frac{d}{dx} f_{j+1/2}(x)$  is  $\frac{1}{\Delta x_j}$  in cell j and  $\frac{-1}{\Delta x_{j+1}}$  in cell j+1

# Leakage Term (continued)

$$\begin{aligned}
 \longrightarrow \quad Term1 &= \int_{\Delta x_j} \frac{d}{dx} [f_{j+1/2}(x) J^\pm(x)] dx - \int_{\Delta x_j} J^\pm(x) \frac{d}{dx} f_{j+1/2}(x) dx \\
 &= f_{j+1/2}(x) J^\pm(x) \Big|_{x_{j-1/2}}^{x_{j+1/2}} - \frac{1}{\Delta x_j} \int_{\Delta x_j} J^\pm(x) dx \\
 &= 1 \cdot J^\pm(x_{j+1/2}) - 0 \cdot J^\pm(x_{j-1/2}) - \frac{1}{\Delta x_j} \int_{\Delta x_j} J^\pm(x) dx \\
 &= J^\pm(x_{j+1/2}) - \frac{1}{\Delta x_j} \int_{\Delta x_j} J^\pm(x) dx
 \end{aligned}$$

$$\longrightarrow \quad Term2 = -J^\pm(x_{j+1/2}) + \frac{1}{\Delta x_{j+1}} \int_{\Delta x_{j+1}} J^\pm(x) dx$$

Summing *Term1* and *Term 2*, cancellation occurs:

$$\pm \int_0^X \int_0^\infty \int_0^{\pm 1} f_{j+1/2}(x) \left[ \mu \frac{d}{dx} \psi(x, \mu, E) \right] d\mu dE dx = \frac{1}{\Delta x_{j+1}} \int_{\Delta x_{j+1}} J^\pm(x) dx - \frac{1}{\Delta x_j} \int_{\Delta x_j} J^\pm(x) dx$$

# Leakage Term (continued)

The boundary cells are handled similarly, but the outgoing and incoming currents on the boundary appear in the equations.

$$F_{j+1/2}^{\pm} \left[ \mu \frac{d}{dx} \psi(x, \mu, E) \right] = \begin{cases} \frac{1}{\Delta x_1} \int_{\Delta x_1} J^{\pm}(x) dx - J^{\pm}(0), & j = 0 \\ \frac{1}{\Delta x_{j+1}} \int_{\Delta x_{j+1}} J^{\pm}(x) dx - \frac{1}{\Delta x_j} \int_{\Delta x_j} J^{\pm}(x) dx, & j = 1, \dots, J-1 \\ J^{\pm}(X) - \frac{1}{\Delta x_J} \int_{\Delta x_J} J^{\pm}(x) dx, & j = J. \end{cases} \quad (6)$$

Some of the current terms  $J^{\pm}(0)$  and  $J^{\pm}(X)$  are known from the boundary conditions.

We have made no approximations in obtaining Eq. (6).

# Result of Applying the Operator

To avoid the messy triple integral notation, let's introduce the following shorthand:

$$\boxed{\langle (\cdot) \rangle_j^\pm = \pm \int_{x_{j-1/2}}^{x_{j+1/2}} \int_0^\infty \int_0^{\pm 1} (\cdot) d\mu dE dx} \quad (7)$$

The result of operating on the transport equation is:  
(corresponding equation for integration over  $\mu < 0$  not shown).

$$\begin{aligned} & \frac{1}{\Delta x_{j+1}} \langle \mu \psi \rangle_{j+1}^+ - \frac{1}{\Delta x_j} \langle \mu \psi \rangle_j^+ + \langle f_{j+1/2} \Sigma_t \psi \rangle_j^+ + \langle f_{j+1/2} \Sigma_t \psi \rangle_{j+1}^+ \\ &= \frac{1}{2} \left[ \langle f_{j+1/2} \Sigma_s \psi \rangle_j^+ + \langle f_{j+1/2} \Sigma_s \psi \rangle_{j+1}^+ + \langle f_{j+1/2} \Sigma_s \psi \rangle_j^- + \langle f_{j+1/2} \Sigma_s \psi \rangle_{j+1}^- \right] + \frac{1}{2} (\mathcal{Q}_{j,1/2} + \mathcal{Q}_{j+1,-1/2}) \end{aligned}$$

*Note: We separated out the spatial integrals so that each term is integrated over only one spatial cell.*

↓

$$\mathcal{Q}_{j,k} = \int_{x_{j-1/2}}^{x_{j+1/2}} \int_0^\infty f_{j+k}(x) Q(x, E) dE dx.$$

(Internal source notation)

# Multiplication by Unity Factor

Recall that we would like equations for the response,

$$R_j^\pm = \pm \int_{x_{j-1/2}}^{x_{j+1/2}} \int_0^\infty \int_0^{\pm 1} r(x, E) \psi(x, \mu, E) d\mu dE dx \equiv \langle r\psi \rangle_j^\pm. \quad (8)$$

Multiply each term by a factor of unity containing the most similar  $R_j^\pm$ .

$$\begin{aligned} & \frac{1}{\Delta x_{j+1}} \left[ \frac{\langle \mu\psi \rangle_{j+1}^+}{\langle r\psi \rangle_{j+1}^+} R_{j+1}^+ - \left[ \frac{1}{\Delta x_j} \frac{\langle \mu\psi \rangle_j^+}{\langle r\psi \rangle_j^+} R_j^+ + \left[ \frac{\langle f_{j+1/2} \Sigma_t \psi \rangle_j^+}{\langle r\psi \rangle_j^+} R_j^+ + \left[ \frac{\langle f_{j+1/2} \Sigma_t \psi \rangle_{j+1}^+}{\langle r\psi \rangle_{j+1}^+} R_{j+1}^+ \right. \right. \right. \right. \quad (9) \\ & = \frac{1}{2} \left( \left[ \frac{\langle f_{j+1/2} \Sigma_s \psi \rangle_j^+}{\langle r\psi \rangle_j^+} R_j^+ + \left[ \frac{\langle f_{j+1/2} \Sigma_s \psi \rangle_{j+1}^+}{\langle r\psi \rangle_{j+1}^+} R_{j+1}^+ + \underbrace{\left[ \frac{\langle f_{j+1/2} \Sigma_s \psi \rangle_j^-}{\langle r\psi \rangle_j^-} R_j^- + \left[ \frac{\langle f_{j+1/2} \Sigma_s \psi \rangle_{j+1}^-}{\langle r\psi \rangle_{j+1}^-} R_{j+1}^- \right]}_{\text{Terms in brackets will become the nonlinear functionals}} \right. \right. \right. \right. \\ & + \frac{1}{2} (\mathcal{Q}_{j,1/2} + \mathcal{Q}_{j+1,-1/2}) \end{aligned}$$

# Functional Definitions

Define the bracketed terms as the following non-linear “functionals”:

$$\mu_j^\pm \equiv \frac{\langle \mu \psi \rangle_j^\pm}{\langle r \psi \rangle_j^\pm} \equiv \frac{\int_{x_{j-1/2}}^{x_{j+1/2}} \int_0^\infty \int_0^{\pm 1} \mu \psi(x, \mu, E) d\mu dE dx}{\int_{x_{j-1/2}}^{x_{j+1/2}} \int_0^\infty \int_0^{\pm 1} r(x, E) \psi(x, \mu, E) d\mu dE dx} \quad (10a)$$

$$\Sigma_{i,j,k}^\pm \equiv \frac{\langle f_{j+k} \Sigma_i \psi \rangle_j^\pm}{\langle r \psi \rangle_j^\pm} \equiv \frac{\int_{x_{j-1/2}}^{x_{j+1/2}} \int_0^\infty \int_0^{\pm 1} f_{j+k}(x) \Sigma_i(x, E) \psi(x, \mu, E) d\mu dE dx}{\int_{x_{j-1/2}}^{x_{j+1/2}} \int_0^\infty \int_0^{\pm 1} r(x, E) \psi(x, \mu, E) d\mu dE dx} \quad (10b)$$

These functionals are simply ratios of various integrals of the angular flux.

We now substitute in the functional notation as well as the following source notation.

$$S_{j,k} = \frac{1}{2} \left( \Delta x_j \Sigma_{s,j,k}^+ R_j^+ + \Delta x_j \Sigma_{s,j,k}^- R_j^- + Q_{j,k} \right) \quad (11)$$

# The Low Order Equations

With Eqs. (10), (11), the **low-order equations and B.C.s** are:

$$\mu_1^\pm R_1^\pm - J^\pm(0) + \Delta x_1 \Sigma_{t,1,-1/2}^\pm R_1^\pm = S_{1,-1/2} \quad (12a)$$

$$\mu_{j+1}^\pm R_{j+1}^\pm - \mu_j^\pm R_j^\pm + \Delta x_j \Sigma_{t,j,1/2}^\pm R_j^\pm + \Delta x_{j+1} \Sigma_{t,j+1,-1/2}^\pm R_{j+1}^\pm = S_{j,1/2} + S_{j+1,-1/2}, \quad (12b)$$

$$1 \leq j \leq J-1$$

$$J^\pm(X) - \mu_J^\pm R_J^\pm + \Delta x_J \Sigma_{t,J,1/2}^\pm R_J^\pm = S_{J,1/2} \quad (12c)$$

$$J^+(0) = -J^-(0) \quad (12d)$$

$$J^-(X) = \int_{-1}^0 \int_0^\infty \mu \psi^R(\mu, E) dE d\mu \quad (12e)$$

**The low-order equations are:**

- Solved with an inexpensive discrete ordinates-like sweep and source iteration
- Exact in space, energy and angle (assuming functionals are known exactly)

# Deterministic Algorithm (like 1GS<sub>2</sub>)

Compute source terms using most recent estimate of  $R_j^\pm$

Start at right boundary:

$$R_j^- = \frac{1}{-\mu_j^- + \Delta x_j \Sigma_{t,j,1/2}^-} \left( -J^-(X) + S_{j,1/2} \right) \quad (13a)$$

Sweep left:

$$R_j^- = \left( \frac{-\mu_{j+1}^- - \Delta x_{j+1} \Sigma_{t,j+1,-1/2}^-}{-\mu_j^- + \Delta x_j \Sigma_{t,j,1/2}^-} \right) R_{j+1}^- + \frac{1}{-\mu_j^- + \Delta x_j \Sigma_{t,j,1/2}^-} \left( S_{j,1/2} + S_{j+1,-1/2} \right) \quad (13b)$$

Turn around at left reflecting boundary:

$$R_1^+ = \left( \frac{-\mu_1^- - \Delta x_1 \Sigma_{t,1,-1/2}^-}{\mu_1^+ + \Delta x_1 \Sigma_{t,1,-1/2}^+} \right) R_1^- + \frac{2}{\mu_1^+ + \Delta x_1 \Sigma_{t,1,-1/2}^+} S_{1,-1/2} \quad (13c)$$

Sweep right:

$$R_{j+1}^+ = \left( \frac{\mu_j^+ - \Delta x_j \Sigma_{t,j,1/2}^+}{\mu_{j+1}^+ + \Delta x_{j+1} \Sigma_{t,j+1,-1/2}^+} \right) R_j^+ + \frac{1}{\mu_{j+1}^+ + \Delta x_{j+1} \Sigma_{t,j+1,-1/2}^+} \left( S_{j,1/2} + S_{j+1,-1/2} \right) \quad (13d)$$

Repeat until converged.

# Monte Carlo Computation of the Functionals

The functionals are *not* known. Simulate the exact problem (including spatial mesh) in continuous energy Monte Carlo.

- Tally all integrals in the numerators and denominators of functionals
- At end of MC simulation, create the set of functionals by taking ratios of these tallies

Modified path length estimators

$$\left. \begin{aligned} & \int_{x_{j-1/2}}^{x_{j+1/2}} \int_0^\infty \int_0^{\pm 1} \mu \psi(x, \mu, E) d\mu dE dx \\ & \int_{x_{j-1/2}}^{x_{j+1/2}} \int_0^\infty \int_0^{\pm 1} f_{j+k}(x) \Sigma_t(x, E) \psi(x, \mu, E) d\mu dE dx \\ & \int_{x_{j-1/2}}^{x_{j+1/2}} \int_0^\infty \int_0^{\pm 1} f_{j+k}(x) \Sigma_s(x, E) \psi(x, \mu, E) d\mu dE dx \end{aligned} \right\} \longrightarrow 10J \text{ tallies}$$

$$\int_{x_{j-1/2}}^{x_{j+1/2}} \int_0^\infty \int_0^{\pm 1} r(x, E) \psi(x, \mu, E) d\mu dE dx \longrightarrow 2J \text{ more tallies per reaction rate desired}$$

Note: This quantity is the desired reaction rate.  
Why do we need to compute the other quantities?

# Why Not Standard Monte Carlo?

**Why do we use Monte Carlo to compute the functionals rather than the desired reaction rate directly?**

We can estimate a ratio of two correlated quantities better than the individual quantities themselves.

**Hypothesis:** For a given number of particles, Monte Carlo estimates of the nonlinear functionals are much more accurate, and have much less variance, than direct Monte Carlo estimates of the desired reaction rates.

Preliminary results indicate the hybrid figure of merit is almost double that of standard Monte Carlo. Therefore, *only about half as many particles are needed for hybrid method.*

# Review

To derive the hybrid method, we:

1. Choose the response function  $r(x, E)$ . For example:

$$r(x, E) = 1 \quad \Rightarrow \quad R = \int_0^\infty \phi dE$$

$$r(x, E) = \Sigma_i(x, E) \quad \Rightarrow \quad R = \int_0^\infty \Sigma_i \phi dE$$

$$r(x, E) = \begin{cases} \Sigma_i(x, E), & E \in E_g \\ 0, & \textit{otherwise} \end{cases} \quad \Rightarrow \quad R = \int_{E_g} \Sigma_i \phi dE$$

2. Multiply the transport equation by a tent function  $f_{j+1/2}(x)$ .
3. Integrate the result over all  $x$  and  $E$ . Then, integrate separately over  $\mu > 0$  and  $\mu < 0$ .
4. Multiply each term by a factor of unity that introduces the reaction rate unknowns.
5. Rearrange the factors in each term to define non-linear “functionals” containing ratios of the unknown angular flux.
6. Estimate these functionals with continuous energy Monte Carlo.
7. Solve the low-order equations for the unknowns using an inexpensive one group,  $S_2$ -like sweep and source iteration.

# Review (continued)

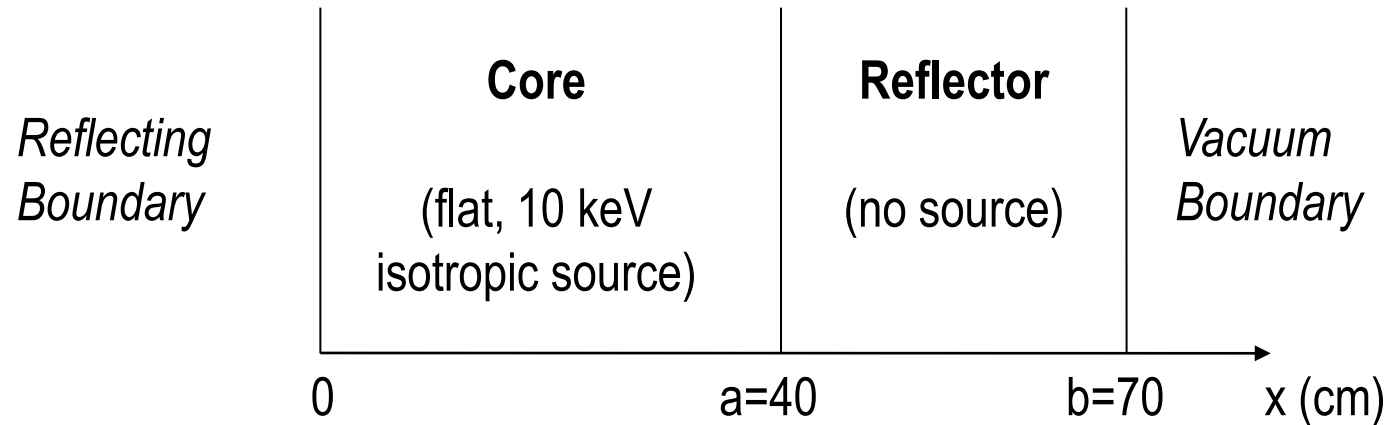
- **Single** reaction rate: **one Monte Carlo calc.** (one set of functionals) and one deterministic calc.
- **Multiple** reaction rates: **one Monte Carlo calc.** (multiple sets of functionals) and multiple deterministic calcs. (inexpensive)
- Calculating multiple reaction rates doesn't increase the expense of the calculation significantly.

## Characteristics of the Hybrid Method

- No energy, angular or spatial approximations were made in deriving these equations.
- The computed result has only statistical error.
- The results of this method satisfy global particle balance.

$$J(X) - J(0) + \int_0^X \int_0^\infty \int_{-1}^1 \Sigma_a(x, E) \psi(x, \mu, E) d\mu dE dx = \int_0^X \int_0^\infty Q(x, E) dE dx$$

# Slab Test Problem

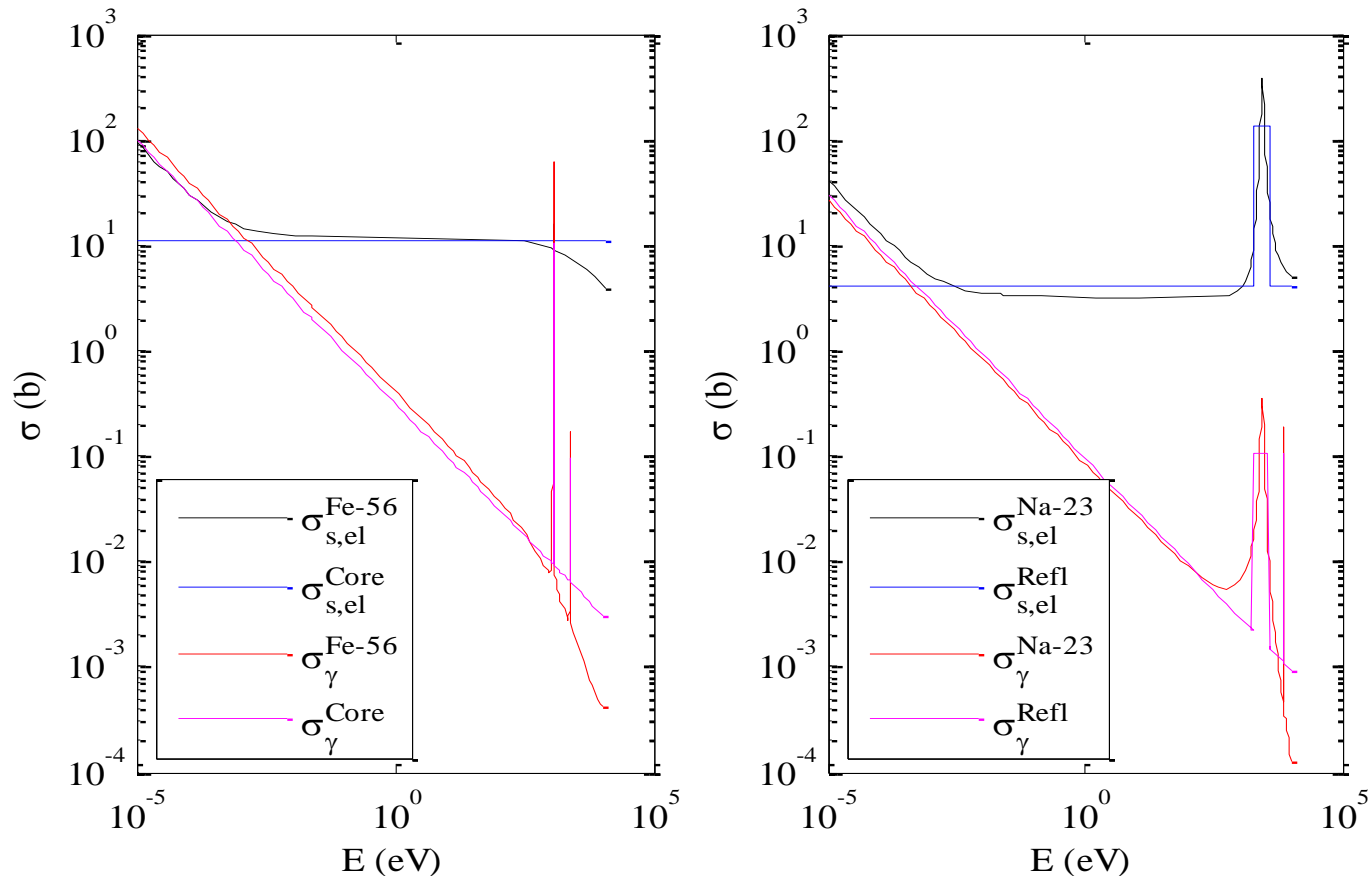


- Core similar to Fe-56 ( $N=0.0848/\text{barn-cm}$ )
- Reflector similar to Na-23 ( $N=0.0254/\text{barn-cm}$ )
- Continuous energy cross sections with resonances approximated by histograms
- Transport effects occur mainly in “resonance” group: 631 eV to 10 keV

Calculate (a) **scalar flux** and (b) **resonance group capture rates** with the hybrid method, multigroup  $S_N$  and standard Monte Carlo

# Test Problem Cross Sections

Fig 1. Comparison of ENDF cross sections with test problem cross sections.



# MGS<sub>N</sub> Calculations

## Multigroup S<sub>N</sub> Overview

- S<sub>16</sub> Gauss-Legendre quadrature
- Groups ranged from coarse to fine (11g, 21g, 51g, 101g, and 251g)
- Equal lethargy groups on [1 eV, 10 keV] plus one group from [0, 1 eV]
- Scalar flux and reaction rates obtained by post-processing group fluxes

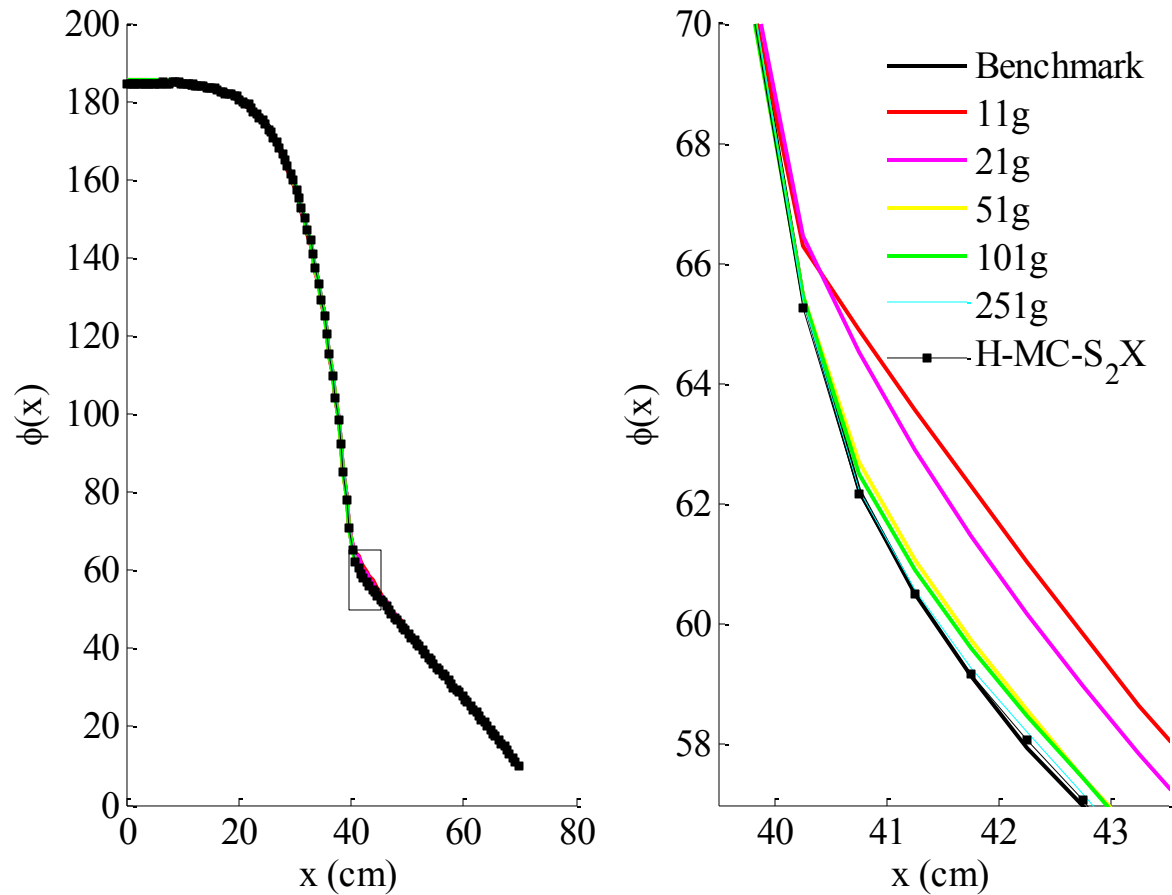
$$\phi_j = \sum_{\forall g} \phi_{g,j} \quad R_j = \sum_{\forall g} \Sigma_{g,j} \phi_{g,j}$$

## Cross Section Condensation

- Consistent with conventional collapsing techniques
- Infinite medium calculation for each material in continuous energy Monte Carlo  
=> Fine group (501g) data  $\Sigma_h, \phi_h$
- Fine group data collapsed to coarser groups

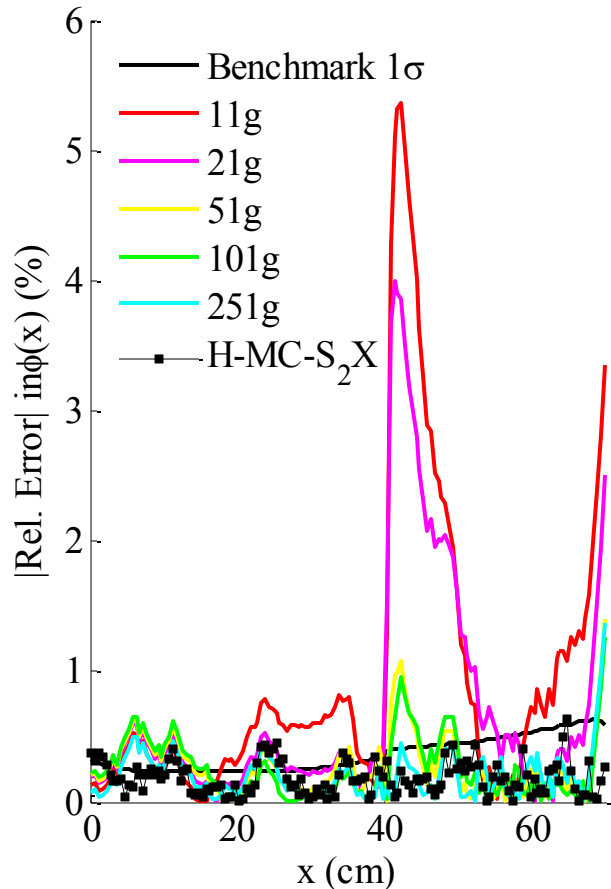
$$\Sigma_g = \frac{\sum_{h \in g} \Sigma_h \phi_h}{\sum_{h \in g} \phi_h}$$

Fig 1.  $\Phi(x)$  across entire slab (left) and near interface (right).  $\Delta x=0.5$  cm.

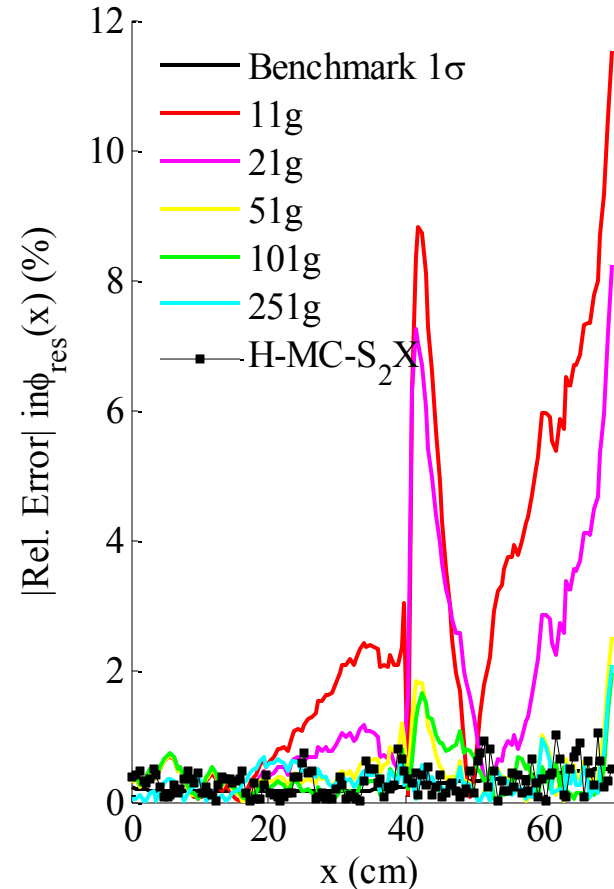


Monte Carlo Histories: Benchmark MC Solution (2e6), H-MC-S<sub>2</sub>X (0.5e6)

**Fig 2. Relative errors in  $\Phi(x)$**



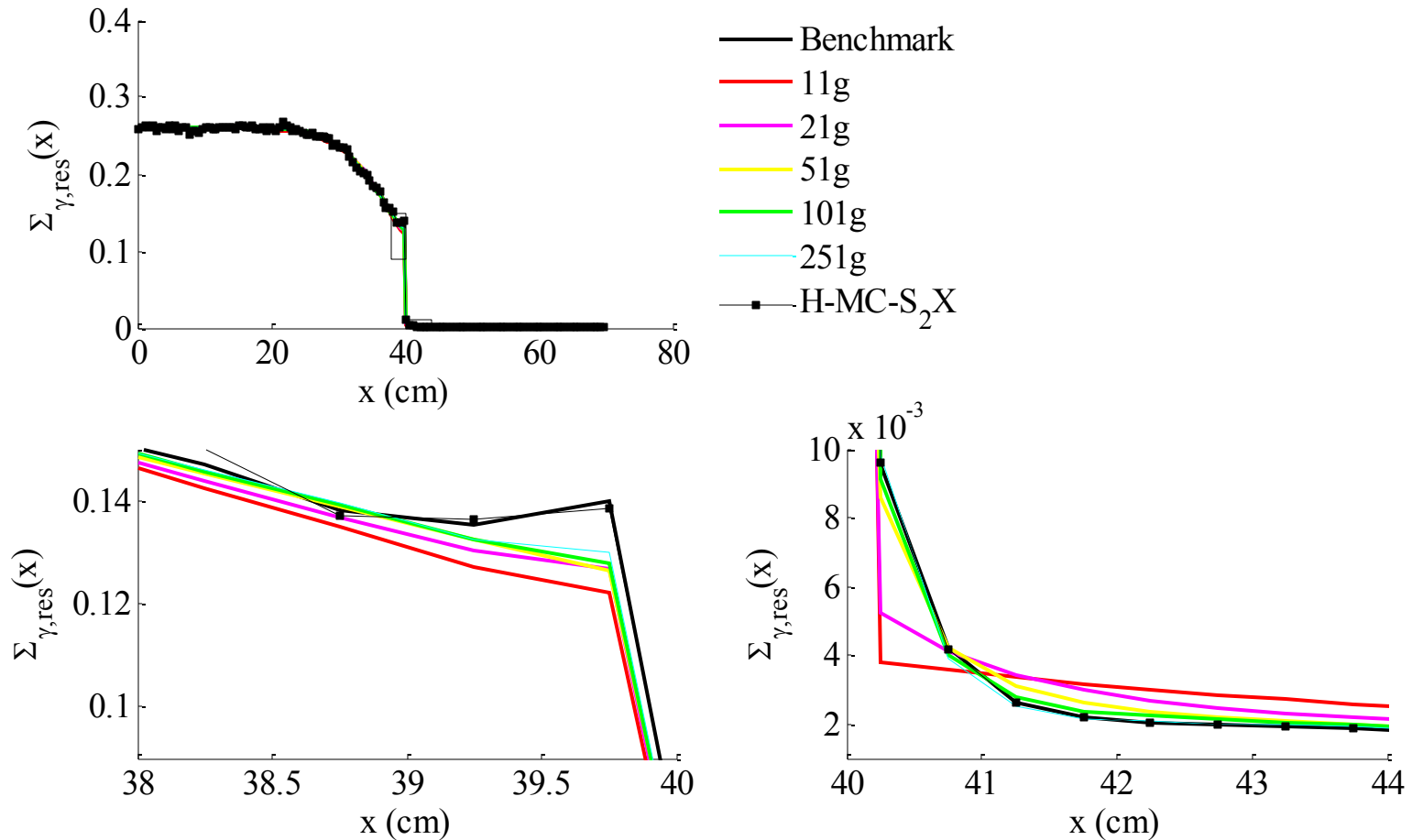
**Fig 3. Relative errors in  $\Phi_{res}(x)$**



**Comments:**

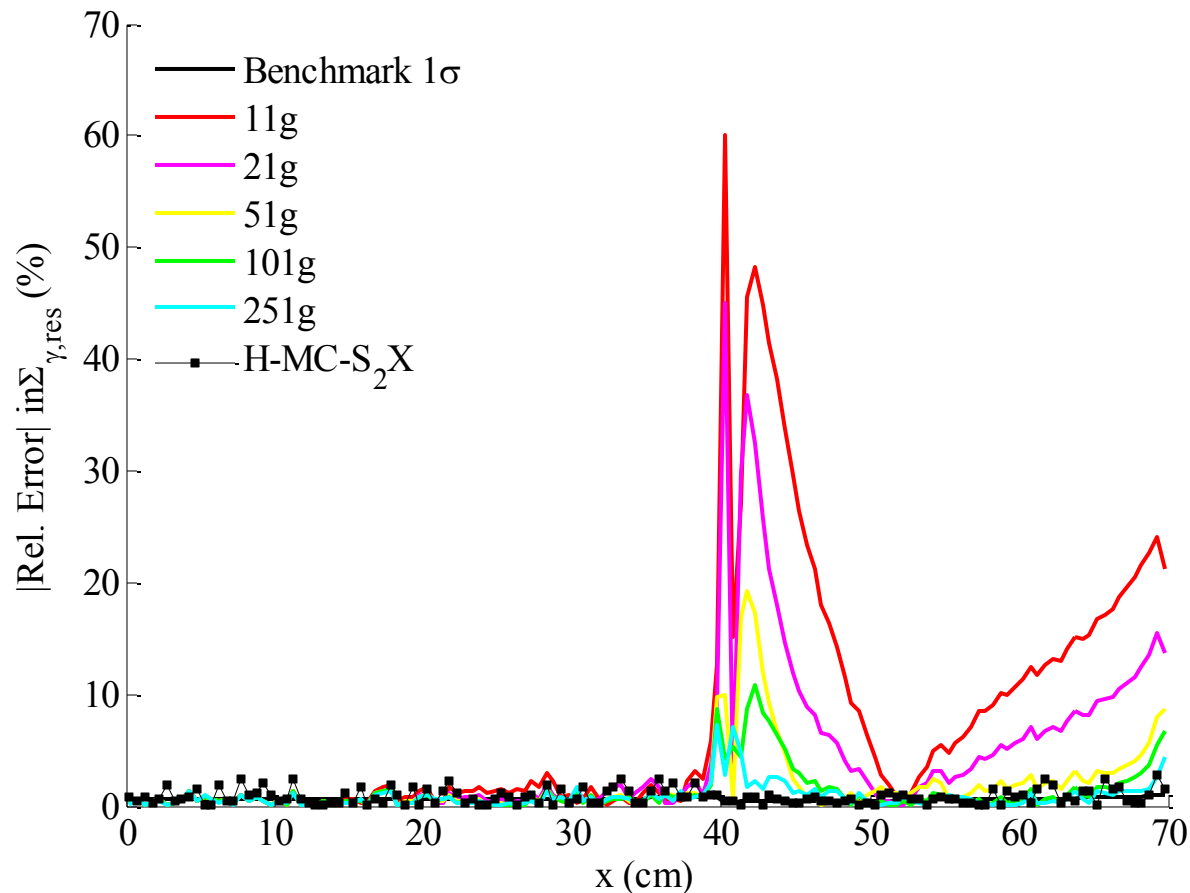
- $MGS_N$  needs 251+ groups to match the accuracy of the 1-group hybrid method near the core-reflector interface ( $x=40$ ) and vacuum boundary ( $x=70$ )
- Resonance group errors twice that of energy integrated flux, as expected

Figure 4.  $\Sigma_{\gamma, \text{res}}(x)$  across slab (resonance group capture rate).  $\Delta x=0.5$  cm.



Monte Carlo Histories: Benchmark MC Solution (4e6), H-MC-S<sub>2</sub>X (1e6)

Figure 4. Relative errors in  $\Sigma_{\gamma, \text{res}}(x)$  compared to benchmark.



**Comments:**

- MGS<sub>N</sub> errors 5-45% near interface; 5-25% near vacuum boundary
- 251+ groups required to match hybrid accuracy near interface and vacuum boundary

## Figure 5. Maximum Relative Errors for Resonance Group Capture Calculation

|               | Max. Rel. Error | Location [cm] | Benchmark 1 $\sigma$ |
|---------------|-----------------|---------------|----------------------|
| <b>11g</b>    | 60.0%           | 40.25         | 0.3%                 |
| <b>21g</b>    | 45.0%           | 40.25         | 0.3%                 |
| <b>51g</b>    | 19.2%           | 41.75         | 0.4%                 |
| <b>101g</b>   | 10.8%           | 42.25         | 0.4%                 |
| <b>251g</b>   | 7.2%            | 39.75         | 0.9%                 |
| <b>HMCS2X</b> | 2.9%*           | 69.25         | 0.9%                 |

\* = Could be further reduced with variance reduction techniques to push neutrons through the slab or by simulating more histories

### Comments:

- Greatest error near interface for deterministic methods
- Deterministic methods suffer from spatial truncation error and transport effects
  - Need to refine both spatial grid and energy groups dramatically to reduce errors
- Errors well outside benchmark statistical bounds
- For hybrid method, greatest error furthest from the source as expected

# Conclusions

**We have developed a new hybrid method that has no truncation error in space, energy or angle.**

- Deterministic calculation similar to one group  $S_2$  with spatially dependent group cross sections
- Uses nonlinear functionals that are estimated with Monte Carlo
- Accurately solves problems with transport effects in energy and angle
- Accurate for problems with strong spatial gradients
- Allows us to study the effects of incorporating angular dependence in problems traditionally solved with MG
- Much more accurate than  $MGS_N$ , which required 250+ groups to capture transport effects for test problem

## **Some difficulties:**

- Error propagation in hybrid methods
- Predicting sensitivity of low order equations to statistical uncertainties in functionals

# Future Work & Acknowledgments

## Future Work

- Extension to eigenvalue problems, anisotropic scattering, and 2-D geom.
- Alternative multigroup cross section generation techniques to determine the effects of including spatial and/or angular dependence
- Could it be possible to estimate the functionals deterministically?
- Test on problems with ray effects

## Funding

This work was partly funded by a United States Department of Energy Nuclear Engineering and Health Physics Fellowship.

## Selected References

1. E. Wolters, et al., "A Hybrid Monte Carlo-S<sub>2</sub> Method for Preserving Neutron Transport Effects," *Proc. M&C*, Saratoga Springs, NY, May 3-7, 2009.
2. G. Aliberti, et al., "Methodologies for Treatment of Spectral Effects at Core-Reflector Interfaces in Fast Neutron Systems," *Proc. PHYSOR*, Chicago, Illinois, April 25-29, 2004.
3. J.F. Lebrat, et al., "Fast Reactor Core-Reflector Interface Effects Revisited," *Proc. PHYSOR*, Seoul, Korea, October 7-10, 2002.

# Hybrid Variance (vs. Standard Monte Carlo)

- ✓ Compare the variance of hybrid and standard MC methods.

To test our previous hypothesis, we computed the figure of merit (FOM) for each method.

- 20 independent estimates of scalar flux with each method (N=50,000; dx=0.5cm)

| Method               | $\sum_{j=1}^J \sigma_j^2$ | $\langle T \rangle$ | $\langle FOM \rangle$ |
|----------------------|---------------------------|---------------------|-----------------------|
| Standard Monte Carlo | 211.7                     | 259.6               | 1.82e-5               |
| Hybrid               | 90.1                      | 335.7               | 3.31e-5               |

$$\langle FOM \rangle = \frac{1}{\left( \sum_{j=1}^J \sigma_j^2 \right) \langle T \rangle}$$


The hybrid figure of merit is almost double that of standard Monte Carlo, so only half as many particles are needed.

**The hybrid method has less variance than standard Monte Carlo.**

# Test Problem Transport Effects

(a) True spectra, (b) infinite medium spectra and (c) true net current from core to reflector.

